Macromolecules

pubs.acs.org/Macromolecules Article

Composition-Driven Structural Modulation and Guest-Induced Nanotemplate Effects of the Host–Guest Complexes Made by a Unimolecular Q-Clip

Jou-Tsen Ou, Tsung-Kai Yang, Heng-Yi Lin, Hong-Yu Hsu, Tzu-Jung Chen, Yi-Sheng Ou, Jia Chen, Cheng-Yu Wang, Bin Sun, and Chien-Lung Wang*

Cite This: *Macromolecules* 2021, 54, 8913–8920 Read Online

ACCESS | Metrics & More | Article Recommendations | Supporting Information

ABSTRACT: The composition of a self-assembly system has long been an essential factor that governs the resulting supramolecular structures. Nevertheless, due to the rigorous demands of structural compatibility in host–guest chemistry, the molar ratio of host–guest mixtures has not been applied as a significant factor in modulating the supramolecular structures of host–guest complexes. In this study, *via* using a novel unimolecular quaternary clip (**Q-clip**) as the host molecule and **pyrene** as the guest molecule and a nanotemplating reagent, we discovered that the changes in the molar ratios of the **Q-clip:pyrene** mixtures resulted in the structural modulation of the host–guest complexes. Supramolecular lamellae made by the 1:4 **Q-clip:pyrene** mixture and a hexagonal columnar phase (Col_h) made by the 1:8 **Q-clip:pyrene** mixture were identified by the 1D powder and 2D fiber WAXS characterizations. Time-resolved synchrotron X-ray characterization and thermal analysis further showed that removing the easily sublimed guest molecules (**pyrene**) *via* thermal annealing simply hollowed out the supramolecular structures without damaging the supramolecular scaffolds made by the **Q-clips**. **Pyrene** is thus a nanotemplating reagent that can be used to create the hollowed-out 2D lamellar and 1D cylindrical scaffolds of **Q-clips**. The study thus gave a novel example of a host–guest mixture that is able to carry out composition-driven structural modulation and guest-induced nanotemplates. The finding broadens the horizon of host–guest chemistry and may inspire more nanoinnovation.

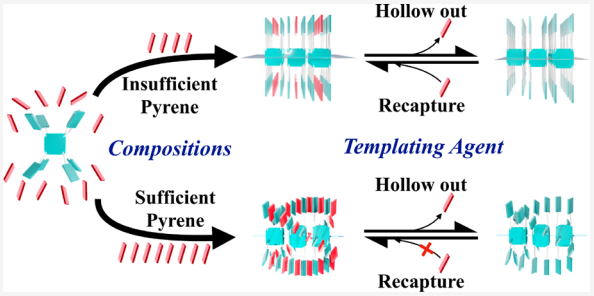

INTRODUCTION

In multicomponent systems, the molar fraction of the constituent components is an essential factor that governs physical properties, physical transitions, and self-assembly of a system.[1] Changes in the molar fractions of the constituent components alter the stabilities of the physical states of a system and result in changes in the self-assembly morphologies.[2−4] For example, manipulating the molar fraction of the constituent components in block copolymers[2] and giant molecules[5,6] has enabled the system to create supramolecular architectures, including 1D nanorods, 2D nanosheets, and 3D interpenetrating networks.[6−8]

Host–guest complexes are a representative bicomponent (or multicomponent) system in supramolecular chemistry. Geometry and symmetry of the constituent components typically determine the final supramolecular structures of the host–guest mixtures since the synthetic host and guest molecules commonly have complementary shapes and can coassemble *via* molecular recognition.[9,10] Particularly, inclusion complexes with polycyclic aromatic hydrocarbons as guest molecules attract great interest to find a way to solve the environmental issue of persistent organic pollutants.[11,12] However, although research studies have shown that linear, trigonal, and tetrahedral guest molecules can assemble with synthetic hosts to give 1D to 3D supramolecular architectures,[13,14] these supramolecular architectures only could form in a specific host–guest composition and cannot be modulated by changing the molar ratio of the host–guest mixtures. There remains no report demonstrating the composition-driven structural modulation of host–guest mixtures to the best of our knowledge.

In addition, the development of porous materials with ordered and tailorable architectures is a subject of intense research.[15] Supramolecules with ordered self-assembly structures and micropores have useful applications in areas such as gas storage, separation, and sensing.[16] Cross-linkable amphiphilic monomers with sacrificial templating molecules have been first used by Kim and co-workers by coassembling them

Received: April 29, 2021
Revised: August 1, 2021
Published: August 12, 2021

Downloaded via SYNCHROTRON RADIATION RESEARCH on February 18, 2022 at 08:30:02 (UTC).
See https://pubs.acs.org/sharingguidelines for options on how to legitimately share published articles.

ACS Publications © 2021 American Chemical Society

https://doi.org/10.1021/acs.macromol.1c00947
Macromolecules 2021, 54, 8913–8920

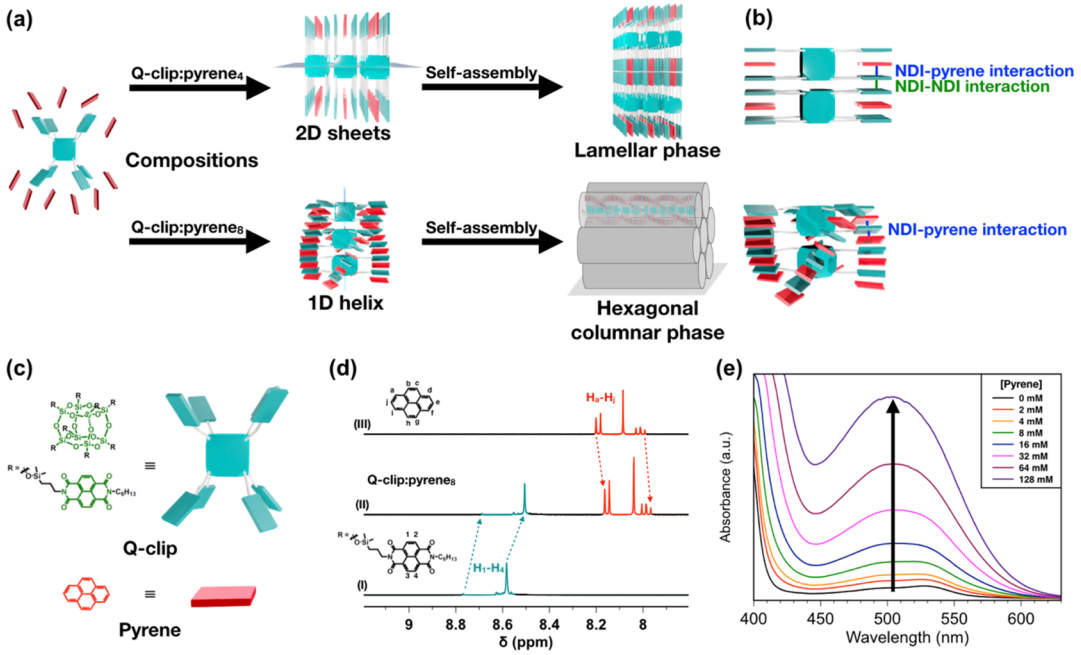

Figure 1. (a) Schematic illustration of the composition-driven structural modulation of the **Q-clip:pyrene** mixtures; (b) the two types of aromatic interactions, **NDI-NDI** and **NDI-pyrene** interactions, in the host–guest complexes. (c) Chemical structures of **Q-clip** and **pyrene**. (d) Partial ^{1}H NMR spectra (400 MHz, 298 K, $CDCl_3$): (I) 1.0 mM **Q-clip**, (II) 1 mM **Q-clip** and 8 mM **pyrene**, and (III) 1.0 mM **pyrene**; (e) UV–vis titration spectra showing the changes in the absorption spectra of **Q-clip** (1 mM) with an increasing concentration of **pyrene** in $CHCl_3$ at 298 K.

into an ordered thermotropic phase and then cross-linking to form the nanoporous host materials after removing the templating molecules.[17] How the presence/absence of guest molecules switch the supramolecular architectures of the host materials has further been extensively studied for the past two decades.[18−20]

Herein, we demonstrate a novel host–guest system, in which the host–guest composition (Figure 1a) can modulate the noncovalent interaction (Figure 1b) in the mixture and thus program the resultant supramolecular architectures. Figure 1c shows the chemical structure of the host molecule, **Q-clip**. It is a unimolecular quaternary clip (**Q-clip**) that owns eight *N*-hexyl-1,4,6,8-naphthalene diimide (**NDI**) as the capture units. Meanwhile, **pyrene** serves as a guest molecule and a nanotemplating reagent to facilitate the charge transfer (CT) interactions and coassemble with the **Q-clip**.[21−24] The types of noncovalent interactions in the **Q-clip:pyrene** mixtures can be adjusted by the composition of the mixture. As shown in Figure 1a,b, both the **NDI-NDI** π-π interaction and **NDI-pyrene** CT interaction are present in the 1:4 **Q-clip:pyrene** mixture (denoted as **Q-clip:pyrene$_4$**), whereas there is only **NDI-pyrene** CT interaction in the1:8 **Q-clip:pyrene** mixture (denoted as **Q-clip:pyrene$_8$**). The balance of the noncovalent interactions in the system was found to be affected by the composition. As a result, structural characterization results show that the **Q-clip:pyrene$_4$** forms a lamellar phase that contains 2D nanosheets of a T_8 cage of polyhedral oligomeric silsesquioxane (POSS) units separated by the layers of the π-stack of the **NDI-pyrene** and **NDI-NDI** mixtures, whereas the **Q-clip:pyrene$_8$** forms a hexagonal columnar phase (Col_h) that contains POSS units stacked into 1D nanorods surrounded by the helices of the **NDI-pyrene** CT complexes. Moreover, **pyrene** can further be used as the nanotemplating reagent to create micropores in templated **Q-clips** because of its low sublimation temperature.[25] The thermal analysis and *in situ* WAXS measurements confirmed that after removing the **pyrene** template by thermal annealing, the templated **Q-clip** maintains the structural integrity of the supramolecular scaffolds and results in the ordered microporous materials. The study thus enables the composition to govern the self-assembly pathways of a host–guest mixture and provide a facile procedure to prepare ordered microporous scaffolds, which broadens the horizons of host–guest chemistry.

RESULTS AND DISCUSSION

The **Q-clip** was synthesized according to Scheme S1. The capture unit, **HA-NDI**, was prepared in two steps. First, monoimidation of 1,4,5,8-naphthalenetetracarboxylic dianhydride (**NDA**) was carried out by reacting **NDA** with hexylamine in dimethyl formamide (DMF) at 110 °C to give **Hex-NMI** in 50% yield. Further reaction of **Hex-NMI** and allylamine in DMF at 110 °C gave **HA-NDI** in 55% yield. Finally, by reacting the excess equivalent of the capture unit (**HA-NDI**) with the core unit (octakis(dimethylsilyloxy)-substituted polyhedral oligomeric silsesquioxanes, **POSS-SiH**) *via* the hydrosilylation reaction, the **Q-clip** was obtained in 45% yield. The products were characterized by ^{1}H NMR, ^{13}C NMR, and mass spectrometry, as shown in Figures S1–S10.

^{1}H NMR titration experiments were performed (Figure 1d) to investigate the host–guest complexation between **Q-clip** and **pyrene** in solution. The **Q-clip:pyrene$_8$** mixtures gave a spectrum that is different from those of pure **Q-clip** and pure **pyrene**, indicating that the fast-exchange process on the NMR time scale did take place due to the CT-complexation of **Q-clip** and **pyrene** molecules in $CDCl_3$ (Figure 1d-II).[26,27] The **NDI** proton signals of **Q-clip** are shifted upfield by 0.08 ppm due to the electron donation from electron-rich **pyrenes**. Meanwhile, the upfield shifts of **pyrene** protons by 0.04 ppm suggest the formation of inclusion complexes *via* catching the **pyrene**

https://doi.org/10.1021/acs.macromol.1c00947
Macromolecules 2021, 54, 8913−8920

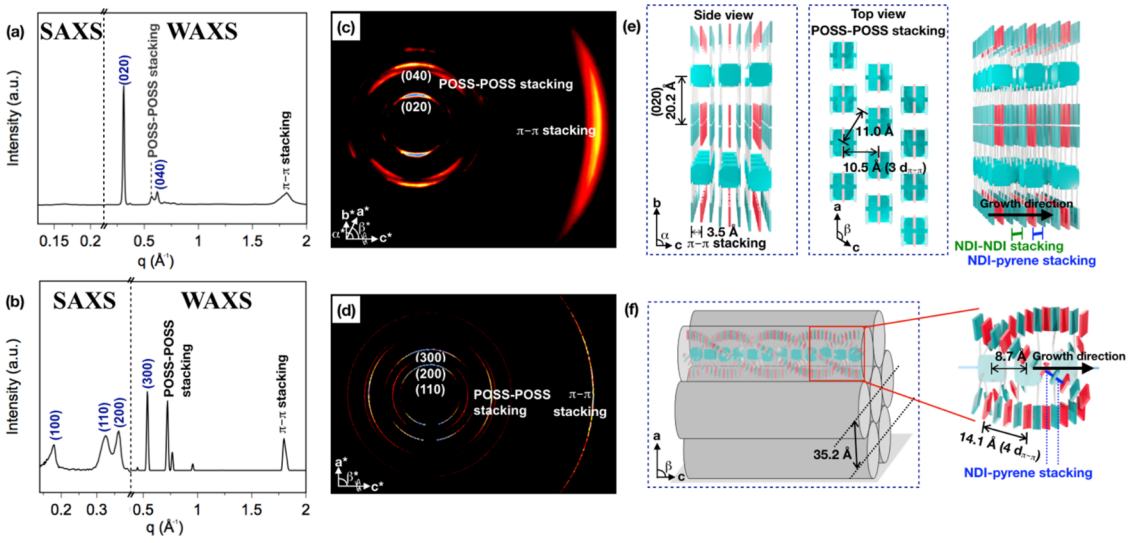

Figure 2. 1D powder SAXS/WAXS patterns of (a) **Q-clip:pyrene**$_4$ and (b) **Q-clip:pyrene**$_8$. The 2D fiber WAXS patterns of (c) **Q-clip:pyrene**$_4$ and (d) **Q-clip:pyrene**$_8$. The lattice models of (e) **Q-clip:pyrene**$_4$ and (f) **Q-clip:pyrene**$_8$.

molecules into the cavities of the **Q-clip** by the **NDI** arms, allowing **pyrene** guests to experience a shielded NMR environment.[28] The existence of CT interactions between the **Q-clip** and **pyrene** was further examined by UV−vis titration experiments (Figure 1e). The spectra of the **Q-clip** solution showed two bands around 490 and 530 nm, respectively. After the addition of **pyrene**, a new broad CT absorption band at 500 nm appeared, indicating the CT-complexation between **Q-clip** and **pyrene**. A continuously increasing intensity of this CT band resulted from the increasing concentration of supramolecular complexes. These results demonstrate that the favorable CT interactions would draw the **Q-clip** and the **pyrene** molecules closer to each other to form supramolecular complexes in solution.

In the condensed phase, noncovalent interactions including **POSS-POSS** interaction, **NDI-NDI** π-π interaction, and **NDI-pyrene** CT interaction coexist in the solid mixture of **Q-clip** and **pyrene**. The balance of different interaction types governs the self-assembly dynamics and the final supramolecular structures. Ideally, to form a complete alternating π-stacking of the **NDI-pyrene** CT complexes, the molar ratio of **NDI** and **pyrene** should be 1:1. Thus, it requires a 1:8 molar ratio of a **Q-clip:pyrene** mixture to provide the necessary condition for the formation of a complete **NDI-pyrene** π-stacking in the mixture, whereas the insufficient supply of **pyrene** results in the presence of both **NDI-NDI** and **NDI-pyrene** π-stacking in the mixture. We thus speculated that changing compositions of the **Q-clip:pyrene** mixtures could alter the aromatic interactions in the system and may result in the composition-driven structural modulation, as illustrated in Figure 1a. To examine the validity of this idea, the self-assembly structures of the 1:4 mixture (**Q-clip:pyrene**$_4$) and 1:8 mixture (**Q-clip:pyrene**$_8$) of the **Q-clip** and **pyrene** were studied by XRD diffractometry. The 1D powder SAXS/WAXS patterns of the two mixtures are shown in Figure 2a,b, respectively. The diffraction patterns of the two mixtures are completely different from those of the pure components (**Q-clip** and **pyrene**) shown in Figures S11 and S12. Two diffraction peaks of **Q-clip:pyrene**$_4$ observed at the scattering vectors (q) = 0.31 and 0.62 Å^{-1} show a q ratio of 2:4, whereas three diffraction peaks of **Q-clip:pyrene**$_8$ observed at q = 0.18, 0.32, and 0.36 Å^{-1} show a q ratio of 1:$\sqrt{3}$:2. The results indicate that **Q-clip:pyrene**$_4$ forms host−guest complexes that self-assembled into a supramolecular lamellar structure, while the host−guest complexes of **Q-clip:pyrene**$_8$ self-assembled into a hexagonal columnar phase (Col$_h$). Note that the electron density of the aromatic domains could be close to the electron density of the POSS domains in the lamellar structure of **Q-clip:pyrene**$_4$, which causes the system absences of the (010) and (030) diffractions. Changing the compositions of the **Q-clip:pyrene** mixtures altered the aromatic interaction in the system and resulted in a rare example of composition-driven structural modulation of host−guest chemistry in the bulk assembly.

To reveal more detailed structures in the mixtures, oriented samples of **Q-clip:pyrene**$_4$ and **Q-clip:pyrene**$_8$ were grown in the apparatus shown in Figure S13 and used to obtain the high-quality 2D fiber WAXS patterns shown in Figure 2c,d. The (020) and (040) diffractions from the lamellar structure of **Q-clip:pyrene**$_4$ and the (200), (110), and (300) diffractions from the Col$_h$ phase of **Q-clip:pyrene**$_8$ were found along the meridian, whereas the diffraction from the π-stacking was found along the equator of the 2D fiber WAXS patterns. The results indicate that the aromatic moieties in the mixtures were π-stacked with a d-spacing of 3.50 Å along the growth axis (c* axis) of the fiber samples. Moreover, perpendicular to the c* axis, the host−guest complexes of **Q-clip:pyrene**$_4$ further stack into a 2D lamellar structure, whereas the supramolecular columns of **Q-clip:pyrene**$_8$ pack into a 2D hexagonal lattice as illustrated in Figure 2e,f. The d-spacing of the lamellar packing (d_{L010}) was deduced to be 40.4 Å from the (020) diffraction found in Figure 2c, and the d-spacing of the hexagonal lattice (d_{H100}) was deduced to be 35.2 Å from the (100) diffraction found in Figure 2b.

An additional diffraction arc of **Q-clip:pyrene**$_4$ was found nearly at the (040) diffraction but deviated slightly from the meridian. This diffraction cannot be incorporated into the b*c* reciprocal lattice. In the seven lattice systems, the monoclinic lattice has its b and c axes perpendicular to each other (α = 90°), but its a and c axes are not perpendicular to each other ($\beta \neq 90°$). Thus, in the 2D fiber diffraction of a monoclinic lattice, when the c* axis is placed along the equator, the b* axis is on the meridian, but the a* axis is deviated from the

https://doi.org/10.1021/acs.macromol.1c00947
Macromolecules 2021, 54, 8913−8920

meridian. Using this crystallographic concept, the unsolved diffraction of **Q-clip:pyrene$_4$** was assigned as the (100) diffraction of the lamellar structure, and d_{L100} was deduced to be 11.0 Å. By combining the structural information along the *a* and *c* axes, the *ac* projection of the lamellar structure was revealed and shown as the "top view" in Figure 2e. More details regarding the correlation between the a^*c^* reciprocal lattice in the 2D WAXS pattern and the *ac* projection of the lattice in real space can be found in Figure S14. It can be found that the POSS core units pack into 2D nanosheets that contain the POSS units separated by 11.0 Å along the *a* axis and 10.5 Å (~3 $d_{\pi\text{-}\pi}$) along the *c* axis.

The structural modulation caused by the additional 4 equiv of **pyrene** can be further investigated by comparing the diffractions from the π-stacking of **Q-clip:pyrene$_4$** and **Q-clip:pyrene$_8$**. The diffraction arc from the π-stacking was found to be much broader in **Q-clip:pyrene$_4$**. By using the Scherrer equation ($L_c = 2\pi K/\Delta_q$, where L_c is the correlation length of a periodic structure, Δ_q is the full width at half-maximum of the π-π diffraction peak, and K is the shape factor (here we use 1.0)), the L_c values of the π-stacking were estimated to be 6.4 nm in **Q-clip:pyrene$_4$** and 18.7 nm in **Q-clip:pyrene$_8$**. Figure S15 provides the illustration that relates the $d_{\pi\text{-}\pi}$ with the L_c and the packing models. In the figure, it can be found that the π-stacking keeps its long-ranged order in average lengths of ca. 18 $d_{\pi\text{-}\pi}$ in the lamellar phase of **Q-clip:pyrene$_4$** and ca. 53 $d_{\pi\text{-}\pi}$ in the Col$_h$ phase of **Q-clip:pyrene$_8$**. In the literature, the **NDI-pyrene** CT complexes were reported to form a face-to-face, alternating π-stacking,[29] which is different from the crystal structure of pure **NDI** that has **NDI-NDI** π-stacking.[30] Since **Q-clip:pyrene$_4$** does not have sufficient equivalent of **pyrene** to form the complete **NDI-pyrene** π-stacking, the broader diffraction arc and the shorter L_c found in **Q-clip:pyrene$_4$** were thus attributed to the presence of the **NDI-NDI** π-stacking, which cut short the correlation length of **NDI-pyrene** π-stacking. On the contrary, **Q-clip:pyrene$_8$** has the correct composition to form the complete and continuous **NDI-pyrene** π-stacking in the mixture. The complete **NDI-pyrene** π-stacking not only resulted in the sharper diffraction arcs but also significantly changed the self-assembly structure of the host–guest complexes. The additional **pyrene** molecules strengthen the aromatic interaction and occupy the extra space in the supramolecular structure, which forbid the formation of the 2D POSS nanosheets found in the lamellar structure of **Q-clip:pyrene$_4$**. Instead, in the Col$_h$ phase of **Q-clip:pyrene$_8$**, 1D POSS nanorods surrounded by the continuous π-stack of **NDI-pyrene** complexes were formed along the growth axis (c^*).

The packing model of **Q-clip:pyrene$_8$** along the c^* axis is also complicated since there are two major diffractions observed along the c^* axis in Figure 2d. The strongest one was assigned as the diffraction from the **NDI-pyrene** π-stacking ($d_{\pi\text{-}\pi}$ = 3.5 Å), and the second one observed at q = 0.72 Å^{-1} was assigned for the 1D **POSS-POSS** stacking ($d_{\text{POSS-POSS}}$ = 8.7 Å). It should be noted that in the continuous **NDI-pyrene** π-stacking, the **pyrene** guest molecules can be placed either within the cavity of a **Q-clip** or between two neighboring **Q-clips**. Thus, for every four steps of π-stacking, the **pyrene** guest molecules will be found to be placed in a similar environment. This may be the reason why one additional weak diffraction at q = 0.44 Å^{-1}, representing a periodicity of 4 $d_{\pi\text{-}\pi}$, was also observed along the equation of Figure 2d. The diffractions of the **POSS-POSS** stacking and continuous **NDI-pyrene** π-stacking were both found on the c^* axis. To accommodate the two types of packings, which have different periodic *d*-spacings ($d_{\text{POSS-POSS}} < 4\ d_{\pi\text{-}\pi}$), the continuous **NDI-pyrene** π-stacking was proposed to twist around the 1D POSS nanorods that contain continuous 1D **POSS-POSS** stacking (Figure 2f). The completely different supramolecular structures of **Q-clip:pyrene$_8$** and **Q-clip:pyrene$_4$** indicate that the 1:8 **Q-clip:pyrene** composition perfects the **NDI-pyrene** π-stacking at the cost of sacrificing the lateral **POSS-POSS** interactions, which degrades the 2D POSS sheet and results in the 1D POSS nanorod in **Q-clip:pyrene$_8$**. In liquid crystal (LC) materials, lamellar structures were found in the smectic phases formed by rod-like mesogens, whereas the columnar phases were reported for discotic mesogens.[31] Nevertheless, formation of both smectic phase and columnar phase by a single type of LC mesogen (rod-like or discotic) is difficult. *Via* the composition-driven structural modulation, the host–guest complexes of **Q-clip:pyrene** were found to behave like a rod-like mesogen to self-assemble into a lamellar structure at the composition of 1:4, while they behave like a discotic mesogen to self-assemble into the Col$_h$ phase. The supramolecular chemistry of the **Q-clip:pyrene** mixture is thus unique among the LC materials and host–guest complexes.

The lamellar and columnar phases of the **Q-clip:pyrene** mixtures can be further hollowed out to create micropores by subliming the **pyrene** guest molecules *via* thermal annealing. In Figure 3a, the thermal gravimetric analysis (TGA) thermo-

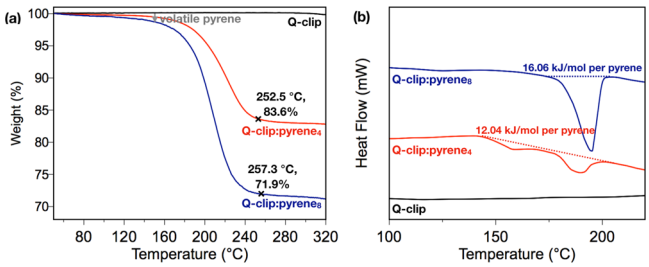

Figure 3. (a) TGA thermograms of **Q-clip**, **Q-clip:pyrene$_4$**, and **Q-clip:pyrene$_8$** recorded at a heating rate of 10 °C min^{-1}; (b) DSC thermograms of **Q-clip**, **Q-clip:pyrene$_4$**, and **Q-clip:pyrene$_8$** recorded at a heating rate of 15 °C min^{-1}.

grams show that the **Q-clip** is thermally stable and has no weight loss in the temperature range from 40 to 300 °C. On the contrary, **pyrene** in the **Q-clip:pyrene** mixtures starts to sublime at around 150 °C, resulting in the 16.7% weight loss for **Q-clip:pyrene$_4$** and 28.1% weight loss for **Q-clip:pyrene$_8$**. The weight loss matches well with the weight percent of **pyrene** in **Q-clip:pyrene$_4$** (16.4%) and **Q-clip:pyrene$_8$** (28.1%), indicating that **pyrene** can be completely removed from the host–guest complexes after the thermal treatment. In Figure 3b, the differential scanning calorimetry (DSC) thermograms show the sublimation temperatures of **pyrene** in the two **Q-clip:pyrene** mixtures and echo the 2D fiber WAXD results in Figure 2c,d because the higher sublimation temperature of **pyrene** in **Q-clip:pyrene$_8$** (193 °C) than in **Q-clip:pyrene$_4$** (160 and 191 °C) suggests that **pyrene** in the complete **NDI-pyrene** CT complex of **Q-clip:pyrene$_8$** is less volatile and more difficult to sublime. Moreover, the two broader and separated endothermic peaks of **Q-clip:pyrene$_4$** suggest that in the lamellar structure, the **pyrene** molecules

https://doi.org/10.1021/acs.macromol.1c00947
Macromolecules 2021, 54, 8913–8920

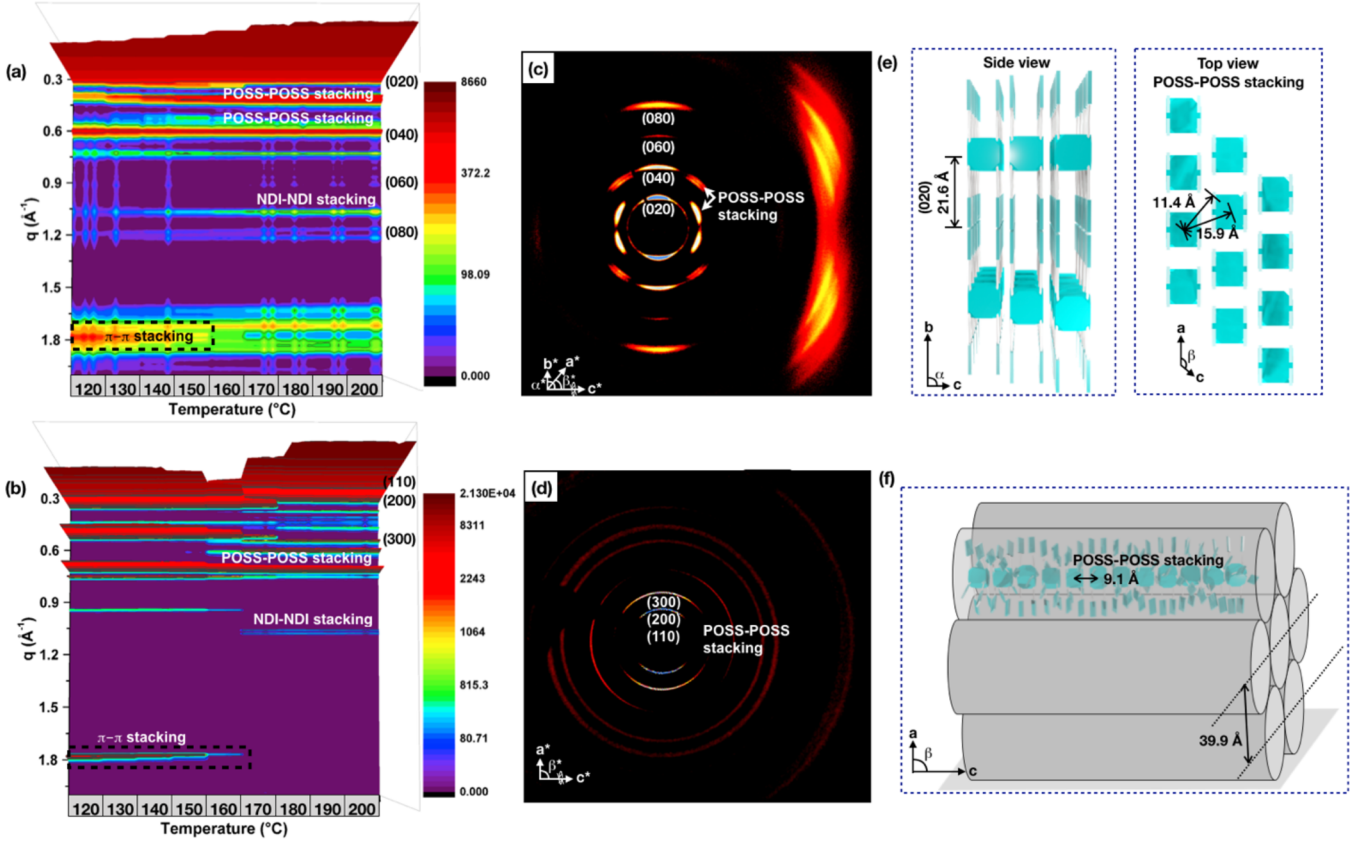

Figure 4. *In situ* WAXS patterns of (a) **Q-clip:pyrene$_4$** and (b) **Q-clip:pyrene$_8$**; 2D WAXS patterns of the (c) **LT Q-clip** and (d) **CT Q-clip**; the lattice model of (e) **LT Q-clip** and (f) **CT Q-clip**.

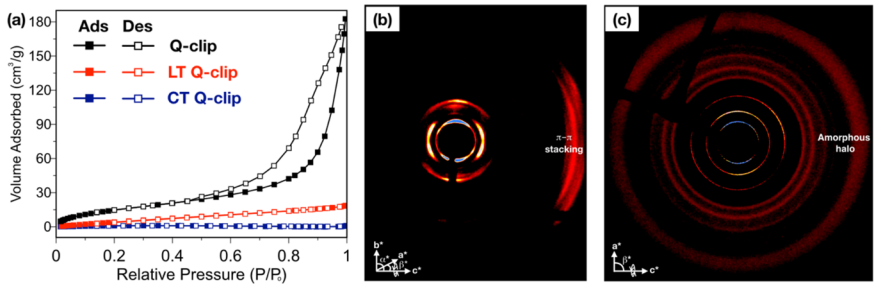

Figure 5. (a) Adsorption (ads) and desorption (des) isotherms of untemplated **Q-clip**, **LT Q-clip**, and **CT Q-clip** at 298 K up to 1 bar for $N_{2(g)}$. 2D WAXS patterns of (b) **LT Q-clip** and (c) **CT Q-clip** after the **pyrene** recapture process.

may be distributed in two different microenvironments, which causes the different volatilities of the **pyrene** guest.

The structural transformation of **Q-clip:pyrene$_4$** and **Q-clip:pyrene$_8$** during the sublimation of **pyrene** was further investigated by the *in situ* WAXS measurements. As shown in Figure 4a,b, the WAXS patterns were recorded when the samples were heated by 15 °C min^{-1} from room temperature. Structural transformations observed from the WAXS patterns become obvious when the sample temperature approaches the sublimation temperature of **pyrene** (ca. 150 °C). The changes in the diffraction patterns indicate that the supramolecular lamellar scaffold of **Q-clip:pyrene$_4$** and columnar scaffold of **Q-clip:pyrene$_8$** remain intact, but the **NDI-pyrene** π-stacking was degraded due to the sublimation of **pyrene** since the diffraction intensities of the (002) and (004) diffractions of **Q-clip:pyrene$_4$** and those of the (200), (110), and (300) diffractions of **Q-clip:pyrene$_8$** were retained, but the diffraction intensity of the π-stacking at q = 1.8 Å^{-1} diminished at temperatures above 160 °C.

Figure 4c,d shows the 2D WAXS patterns of the thermally annealed **Q-clip:pyrene$_4$** and **Q-clip:pyrene$_8$** after annealing at 140 °C under vacuum for 12 h. The two samples now contain no **pyrene** but still keep clear (020), (040), (060), and (080) diffractions from the lamellar scaffold and clear (200), (110), and (300) diffractions from the columnar scaffold. Although the removal of **pyrene** caused the expansion of the lamellar *d*-spacing (d_{L010}) to 43.2 Å and the hexagonal lattice (d_{H100}) to 39.9 Å (illustrated in Figure 4e,f), the 2D WAXS patterns further prove that the **Q-clip** can maintain the supramolecular scaffolds after removing **pyrene**. The two thermally annealed samples thus can be considered as the "lamella-templated **Q-clip** (**LT Q-clip**)" and "column-templated **Q-clip** (**CT Q-clip**)" prepared *via* hollowing out the lamellar structure of the **Q-clip:pyrene$_4$** and the Col$_h$ structure of the **Q-clip:pyrene$_8$**,

https://doi.org/10.1021/acs.macromol.1c00947
Macromolecules 2021, 54, 8913−8920

respectively. In the 2D WAXS patterns, it is also evident that at the equator, the diffraction intensity from the π-stacking of the two samples has significantly decayed because there are no more **NDI-pyrene** CT complexes to give a periodic *d*-spacing of 3.50 Å. Nevertheless, the periodic structures made by the 2D and 1D stack of the POSS units are retained because similar to **Q-clip:pyrene$_4$**, the **LT Q-clip** gave an additional diffraction next to its (040) diffraction (*d*-spacing = 11.4 Å, see Figure 4c), and just like **Q-clip:pyrene$_8$**, the **CT Q-clip** delivers the diffraction of **POSS-POSS** stacking along the equator (see Figure 4d). An additional diffraction of the **LT Q-clip** next to the (020) diffraction has a *d*-spacing of 15.9 Å and is assumed to be the diagonal **POSS-POSS** distance as illustrated in Figure 4e. Thus, the noncovalent interaction among the POSS units of the **Q-clips** may allow the **Q-clip** molecules to maintain the structural integrity of the lamellar and columnar supramolecular scaffolds, while the sublimation of **pyrene** hollows out the host−guest complexes and makes **pyrene** a nanotemplating reagent.

Because the templated **Q-clips** were supposed to contain micropores in their aromatic domains after removing the **pyrene** templating reagent, we further investigated the porosity of templated **Q-clips** and **Q-clip** *via* nitrogen adsorption/desorption analysis (Figure 5a). While the N_2 isotherm curve of the untemplated **Q-clip** revealed much higher absorbed volume of $N_{2(g)}$ and possessed mesopores with a broad pore size distribution at 45 nm (Figure S16), both the adsorption capacity of **LT Q-clip** and **CT Q-clip** declined dramatically. These results indicated that **Q-clip** formed more compact structures after it was lamella- or column-templated. Considering that the sublimation of **pyrene** from the **NDI-pyrene** CT complexes may only leave rectangular holes with a pore size less than 1 nm and a shape similar to **pyrene**, it is reasonable that the micropores in the templated **Q-clips** were not measured by the nitrogen adsorption/desorption experiment. Nevertheless, the ordered micropores in the templated **Q-clips** seem to be revealed by the *in situ* WAXS patterns (Figure 4a,b), as a new diffraction peak with a *d*-spacing of 5.9 Å appeared when the diffraction of the π-stacking at q = 1.8 Å^{-1} diminished due to the removal of **pyrene** at temperatures above 150−160 °C. The periodicity of 5.9 Å could come from the averaged distance of the **NDI** units in the templated **Q-clips** after the removal of **pyrene**. The periodicity is big enough to accommodate π-conjugated guests, so the templated **Q-clips** may act like a nanobookshelf that can store π-conjugated guests into its ordered micropores. To validate this possibility, both **LT Q-clip** and **CT Q-clip** were stored in a glass vial that contained vaporized **pyrene** molecules for 4 days (the apparatus is shown in Figure S17). The reappearance of the diffraction at q = 1.8 Å^{-1} on the equator of the 2D WAXS patterns shown in Figure 5b confirmed that the **LT Q-clip** can retake the vaporized **pyrene** guests to restore the **NDI-pyrene** π-stacking. Thus, the **LT Q-clip** is similar to a nanobookshelf that contained ordered micropores with a pore size less than 1 nm. In contrast, the diffraction of the **NDI-pyrene** π-stacking was not restored in the **CT Q-clip** after the same procedure, indicating that the structure of the **CT Q-clip** was too compact for the re-entry of the **pyrene** guests.

CONCLUSIONS

In this work, we achieved composition-driven structural modulation and prepared lamella-templated and column-templated microporous scaffolds *via* simply coassembling and thermal annealing the mixtures of a novel host (**Q-clip**) and a sublimable guest (**pyrene**). Changing the compositions of the **Q-clip:pyrene** mixture was examined as the key factor to manipulate the balance of the noncovalent interactions and consequently the final supramolecular structures of the host−guest mixtures. The supramolecular structures were characterized by 1D powder SAXS/WAXS and 2D fiber WAXS. It was found that the insufficient supply of **pyrene** resulted in the incomplete formation of the **NDI-pyrene** CT complexes, and consequently, the 1:4 mixture (**Q-clip:pyrene$_4$**) formed a lamellar phase that contained the 2D nanosheets of POSS units. In contrast, the sufficient supply of **pyrene** resulted in the complete formation of the **NDI-pyrene** CT complexes, so the 1:8 mixture (**Q-clip:pyrene$_8$**) formed a Col_h phase that contained the 1D nanorods of POSS units. Moreover, the TGA, DSC, and *in situ* WAXS results indicated that the **Q-clip** in **Q-clip:pyrene$_4$** and **Q-clip:pyrene$_8$** can maintain the structural integrity of the supramolecular scaffolds while **pyrene** sublimes away from the host−guest complexes. The sublimation process thus hollowed out the lamellar structure of the **Q-clip:pyrene$_4$** and the Col_h phase of the **Q-clip:pyrene$_8$** and left the **LT Q-clip** and **CT Q-clip** behind as the ordered microporous lamellar and columnar scaffolds. The 2D WAXS results further revealed that **LT Q-clip** acted like a nanobookshelf that could reload **pyrene** into its micropores, while the structure of the **CT Q-clip** was too compact for **pyrene** to enter its micropores. The unique coassembly behaviors of the **Q-clip:pyrene** mixtures thus make composition an important and useful factor to diversify the supramolecular structures of host−guest complexes. Moreover, taking advantage of the robust supramolecular scaffolds and the easily sublimed guest, our study also provides a facile nanotemplating technique for the further development of ordered microporous materials.

ASSOCIATED CONTENT

Supporting Information

The Supporting Information is available free of charge at https://pubs.acs.org/doi/10.1021/acs.macromol.1c00947.

Complete descriptions of experimental procedures, including the synthesis of **Q-clip**, X-ray structure determination, and illustration of sample preparation methods (PDF)

AUTHOR INFORMATION

Corresponding Author

Chien-Lung Wang − *Department of Applied Chemistry, National Yang Ming Chiao Tung University (National Chiao Tung University), Hsinchu 30010, Taiwan;* orcid.org/0000-0002-5977-2836; Email: kclwang@nctu.edu.tw

Authors

Jou-Tsen Ou − *Department of Applied Chemistry, National Yang Ming Chiao Tung University (National Chiao Tung University), Hsinchu 30010, Taiwan*

Tsung-Kai Yang − *Department of Applied Chemistry, National Yang Ming Chiao Tung University (National Chiao Tung University), Hsinchu 30010, Taiwan*

Heng-Yi Lin − *Department of Applied Chemistry, National Yang Ming Chiao Tung University (National Chiao Tung University), Hsinchu 30010, Taiwan*

https://doi.org/10.1021/acs.macromol.1c00947
Macromolecules 2021, 54, 8913−8920

Hong-Yu Hsu − *Department of Applied Chemistry, National Yang Ming Chiao Tung University (National Chiao Tung University), Hsinchu 30010, Taiwan*
Tzu-Jung Chen − *Department of Applied Chemistry, National Yang Ming Chiao Tung University (National Chiao Tung University), Hsinchu 30010, Taiwan*
Yi-Sheng Ou − *Department of Materials Science and Engineering, National Yang Ming Chiao Tung University (National Chiao Tung University), Hsinchu 30010, Taiwan*
Jia Chen − *State Key Laboratory for Modification of Chemical Fibers and Polymer Materials, College of Materials Science and Engineering, Donghua University, Shanghai 201620, P. R. China*
Cheng-Yu Wang − *Department of Materials Science and Engineering, National Yang Ming Chiao Tung University (National Chiao Tung University), Hsinchu 30010, Taiwan;* orcid.org/0000-0002-9238-6582
Bin Sun − *State Key Laboratory for Modification of Chemical Fibers and Polymer Materials, College of Materials Science and Engineering, Donghua University, Shanghai 201620, P. R. China*

Complete contact information is available at: https://pubs.acs.org/10.1021/acs.macromol.1c00947

Author Contributions

All authors have given approval to the final version of the manuscript.

Funding

This work was supported in part by the Ministry of Science and Technology, Taiwan (MOST 109-2223-E-009-001-MY3) and State Key Laboratory for Modification of Chemical Fibers and Polymer Materials, Donghua University.

Notes

The authors declare no competing financial interest.

■ ACKNOWLEDGMENTS

SAXS experiments and *in situ* WAXS experiments were performed on Taiwan beamlines at the National Synchrotron Radiation Center (BL23A1 and 13A1).

■ REFERENCES

(1) Cheng, S. Z. D.; Keller, A. The Role of Metastable States in Polymer Phase Transitions: Concepts, Principles, and Experimental Observations. *Annu. Rev. Mater. Sci.* **1998**, *28*, 533−562.
(2) Bates, F. S.; Fredrickson, G. H. Block Copolymers—Designer Soft Materials. *Phys. Today* **1999**, *52*, 32−38.
(3) Hu, H.; Gopinadhan, M.; Osuji, C. O. Directed Self-Assembly of Block Copolymers: a Tutorial Review of Strategies for Enabling Nanotechnology with Soft Matter. *Soft Matter* **2014**, *10*, 3867−3889.
(4) Bates, F. S. Block Copolymers Near the Microphase Separation Transition. 2. Linear Dynamic Mechanical Properties. *Macromolecules* **1984**, *17*, 2607−2613.
(5) Zhang, W.; Lu, X.; Mao, J.; Hsu, C.-H.; Mu, G.; Huang, M.; Guo, Q.; Liu, H.; Wesdemiotis, C.; Li, T.; Zhang, W.-B.; Li, Y.; Cheng, S. Z. D. Sequence-Mandated, Distinct Assembly of Giant Molecules. *Angew. Chem., Int. Ed.* **2017**, *56*, 15014−15019.
(6) Zhang, W.; Zhang, S.; Guo, Q.; Lu, X.; Liu, Y.; Mao, J.; Wesdemiotis, C.; Li, T.; Li, Y.; Cheng, S. Z. D. Multilevel Manipulation of Supramolecular Structures of Giant Molecules via Macromolecular Composition and Sequence. *ACS Macro Lett.* **2018**, *7*, 635−640.
(7) Barboiu, M.; Lehn, J.-M. Dynamic Chemical Devices: Modulation of Contraction/Extension Molecular Motion by Coupled-Ion Binding/pH Change-Induced Structural Switching. *Proc. Natl. Acad. Sci.* **2002**, *99*, 5201−5206.
(8) Wu, S.-L.; Hong, C.-Y.; Wu, K.-Y.; Lan, S.-T.; Hsieh, C.-T.; Chen, H.-L.; Wang, C.-L. Conformational Preferences and the Phase Stability of Fullerene Hexa-Adducts. *Chem. − Asian J.* **2016**, *11*, 2011−2015.
(9) Vinciguerra, B.; Zavalij, P. Y.; Isaacs, L. Synthesis and Recognition Properties of Cucurbit[8]Uril Derivatives. *Org. Lett.* **2015**, *17*, 5068−5071.
(10) Guo, F.; Sun, Y.; Xi, B.; Diao, G. Recent Progress in the Research on the Host−guest Chemistry of Pillar[N]Arenes. *Supramol. Chem.* **2018**, *30*, 81−92.
(11) Teresa Albelda, M.; Frías, J. C.; García-España, E.; Schneider, H.-J. Supramolecular complexation for environmental control. *Chem. Soc. Rev.* **2012**, *41*, 3859−3877.
(12) Morillo, E.; Antonia Sánchez-Trujillo, M.; Ramon Moyano, J.; Villaverde, J.; Eulalia Gómez-Pantoja, M.; Ignacio Pérez-Martínez, J. Enhanced Solubilisation of Six PAHs by Three Synthetic Cyclodextrins for Remediation Applications: Molecular Modelling of the Inclusion Complexes. *PLoS One* **2012**, *7*, e44137.
(13) Tian, J.; Wang, H.; Zhang, D.-W.; Liu, Y.; Li, Z.-T. Supramolecular Organic Frameworks (SOFs): Homogeneous Regular 2D and 3D Pores in Water. *Natl. Sci. Rev.* **2017**, *4*, 426−436.
(14) Yang, L.; Tan, X.; Wang, Z.; Zhang, X. Supramolecular Polymers: Historical Development, Preparation, Characterization, and Functions. *Chem. Rev.* **2015**, *115*, 7196−7239.
(15) Brunauer, S.; Emmett, P. H.; Teller, E. Adsorption of Gases in Multimolecular Layers. *J. Am. Chem. Soc.* **1938**, *60*, 309−319.
(16) Chen, B.; Xiang, S.; Qian, G. Metal−Organic Frameworks with Functional Pores for Recognition of Small Molecules. *Acc. Chem. Res.* **2010**, *43*, 1115−1124.
(17) Lee, H.-K.; Lee, H.; Ko, Y. H.; Chang, Y. J.; Oh, N.-K.; Zin, W.-C.; Kim, K. Synthesis of a Nanoporous Polymer with Hexagonal Channels From Supramolecular Discotic Liquid Crystals. *Angew. Chem., Int. Ed.* **2001**, *40*, 2669−2671.
(18) Ishida, Y.; Amano, S.; Iwahashi, N.; Saigo, K. Switching of Structural Order in a Cross-Linked Polymer Triggered by the Desorption/Adsorption of Guest Molecules. *J. Am. Chem. Soc.* **2006**, *128*, 13068−13069.
(19) Bhattacharjee, S.; Lugger, J. A. M.; Sijbesma, R. P. Tailoring Pore Size and Chemical Interior of Near 1 Nm Sized Pores in a Nanoporous Polymer Based on a Discotic Liquid Crystal. *Macromolecules* **2017**, *50*, 2777−2783.
(20) Concellón, A.; Schenning, A. P. H. J.; Romero, P.; Marcos, M.; Serrano, J. L. Size-Selective Adsorption in Nanoporous Polymers From Coumarin Photo-Cross-Linked Columnar Liquid Crystals. *Macromolecules* **2018**, *51*, 2349−2358.
(21) Yang, T.-K.; Ou, J.-T.; Lin, H.-Y.; Peng, W.-C.; Jao, M.-H.; Chen, J.; Sun, B.; Zhu, Y.; Wang, C.-L. Adaptive Molecular Quaternary Clips Made with Pyrene Functionalized Polyhedral Oligomeric Silsesquioxane. *Nanoscale Adv.* **2021**, *3*, 173−176.
(22) Wang, K.; Guo, Z.; Zhang, L.; Sun, K.; Yu, P.; Zhou, S.; Wang, W.; Li, Z. Co-Assembly of Donor and Acceptor Towards Organogels Tuned by Charge Transfer Interaction Strength. *Soft Matter* **2017**, *13*, 1948−1955.
(23) Yeh, M.-Y.; Lin, H.-C. Theoretical Analysis of the Intermolecular Interactions in Naphthalene Diimide and Pyrene Complexes. *Phys. Chem. Chem. Phys.* **2014**, *16*, 24216−24222.
(24) Chen, J.; Lin, H.-Y.; Ji, X.; Zhao, H.; Sun, B.; Wang, C.-L.; Zhu, M. Host−Guest Chemistry of Giant Molecular Shape Amphiphiles Based on POSS−PDI Conjugates. *Nanoscale* **2021**, *13*, 4295−4300.
(25) Roux, M. V.; Temprado, M.; Chickos, J. S.; Nagano, Y. Critically Evaluated Thermochemical Properties of Polycyclic Aromatic Hydrocarbons. *J. Phys. Chem. Ref. Data* **2008**, *37*, 1855−1996.
(26) Zhang, Z.; Liang, H.; Li, M.; Shao, L.; Hua, B. Host−Guest Complexation of Perethylated Pillar[6]Arene Toward Ferrocene Derivatives Both in Solution and Solid State: Different Binding

Modes Induced by Minor Structural Changes of Guests. *Org. Lett.* **2020**, *22*, 1552−1556.
(27) Dai, D.; Li, Z.; Yang, J.; Wang, C.; Wu, J.-R.; Wang, Y.; Zhang, D.; Yang, Y. W. Supramolecular Assembly-Induced Emission Enhancement for Efficient Mercury(II) Detection and Removal. *J. Am. Chem. Soc.* **2019**, *141*, 4756−4763.
(28) Tamanini, E.; Ponnuswamy, N.; Pantoş, G. D.; Sanders, J. K. M. New Host−Guest Chemistry of Supramolecular Nanotubes. *Faraday Discuss.* **2010**, *145*, 205−218.
(29) Kumar, N. S. S.; Gujrati, M. D.; Wilson, J. N. Evidence of Preferential π-Stacking: a Study of Intermolecular and Intramolecular Charge Transfer Complexes. *Chem. Commun.* **2010**, *46*, 5464−5466.
(30) Keeling, D. L.; Oxtoby, N. S.; Wilson, C.; Humphry, M. J.; Champness, N. R.; Beton, P. H. Assembly and Processing of Hydrogen Bond Induced Supramolecular Nanostructures. *Nano Lett.* **2003**, *3*, 9−12.
(31) Wunderlich, B. *Thermal Analysis of Polymeric Materials*; SpringerVerlag: New York, 2005; DOI: 10.1007/b137476.

https://doi.org/10.1021/acs.macromol.1c00947
Macromolecules 2021, 54, 8913−8920